JGR Planets

RESEARCH ARTICLE
10.1029/2023JE008279

Special Section:
The Frontiers in Jupiter Science and Exploration

On the Global Features of the 10–60-Min ULF Waves in Jovian Magnetosphere: Juno Observations

J. W. Sun[1], L. Xie[1], Z. H. Yao[2,3,4,5], S. Y. Fu[1], W. R. Dunn[5], D. Grodent[6], B. Bonfond[6], B. Zhang[2], D. X. Pan[7], Y. Xu[3,4], and Y. N. Chen[8]

[1]School of Earth and Space Sciences, Peking University, Beijing, China, [2]Department of Earth Sciences, University of Hong Kong, Pokfulam, China, [3]Key Laboratory of Earth and Planetary Physics, Institute of Geology and Geophysics, Chinese Academy of Sciences, Beijing, China, [4]College of Earth and Planetary Sciences, University of Chinese Academy of Sciences, Beijing, China, [5]Department of Physics and Astronomy, University College London, London, UK, [6]Laboratoire de Physique Atmosphérique et Planétaire, STAR Institute, Université de Liège, Liège, Belgium, [7]School of Geophysics and Information Technology, China University of Geosciences (Beijing), Beijing, China, [8]Department of Earth and Space Sciences, Southern University of Science and Technology, Shenzhen, China

Key Points:

- We investigate the spatial distribution and periodic characteristics of ultra-low frequency (ULF) waves in the Jovian magnetosphere
- We examine and compare the occurrence rate of ULF waves under different solar wind compression states
- The connection between ULF waves and auroral morphology provides key constraints on wave generation mechanisms

Correspondence to:
L. Xie and Z. H. Yao,
xielun@pku.edu.cn;
yaozh@hku.hk

Citation:
Sun, J. W., Xie, L., Yao, Z. H., Fu, S. Y., Dunn, W. R., Grodent, D., et al. (2024). On the global features of the 10–60-min ULF waves in Jovian magnetosphere: Juno observations. *Journal of Geophysical Research: Planets*, *129*, e2023JE008279. https://doi.org/10.1029/2023JE008279

Received 5 JAN 2024
Accepted 7 MAR 2024

Abstract In the Jovian magnetosphere, quasi-periodic phenomena, with quasi-periods on the order of 10–60 min, are frequently identified using different data sets. These pulsations are a branch of ultra-low frequency (ULF) waves, which are believed to play a crucial role in driving the energy circulation within Jupiter's magnetosphere. In this study, we utilize magnetic field data collected by Juno between 2016 and 2022 to perform a comprehensive global statistical analysis of the spatial distribution and periodic characteristics of ULF waves in the Jovian magnetosphere. Our findings reveal distinct periodic features observed at different latitudes and distances, providing valuable insights into the generation mechanisms of ULF waves. Furthermore, we establish a close relationship between the presence of these ULF wave fluctuations and the magnetospheric state, such as under conditions of solar wind compression. By combining contemporaneous ultraviolet aurora observations from the Hubble Space Telescope (HST) and magnetic field data obtained by Juno, we have discovered that the compressed magnetospheres exhibit more pronounced ULF waves and enhanced auroral activity. These results provide a global picture of the distribution, implying potential generation of ULF waves in the Jovian magnetosphere, and shedding light on the processes behind the 10–60-min energy releases.

Plain Language Summary In the Jovian system, there are patterns of magnetic waves with periods of 10–60 min. These waves are part of a larger category called ultra-low-frequency waves and play an important role in how energy moves around Jupiter. Here, we study these waves using data collected by the Juno spacecraft from 2016 to 2022, investigating where these waves occur and how often they occur. The waves are different depending on the location and distance from Jupiter, which gives us clues about how they are created. These waves also appear to be more common when Jupiter's magnetic field is compressed by the solar wind. We have also combined data from the Hubble Space Telescope and Juno, and found that the compressed magnetic field leads to more of these waves and stronger auroras on Jupiter. This research helps us to understand how these 10–60-min bursts of energy work in Jupiter's magnetosphere.

1. Introduction

Jupiter's rapidly rotating magnetic field imparts strong electromagnetic forces on the surrounding plasma in the magnetosphere, leading to complicated particle acceleration and mass circulation. The primary source of particles in the Jovian magnetosphere is from the volcanic activity of its closest moon Io. As these charged particles are diffusing outward, they are constrained by the centrifugal force near the equatorial plane (Bagenal et al., 2016), and eventually stretch the magnetic field lines forming a magnetodisk. Within the vast Jovian magnetosphere, ultra-low-frequency (ULF) waves are abundant (Lysak, 2022; Lysak & Song, 2020; Manners & Masters, 2020). These waves play a crucial role in energy dissipation within the magnetosphere-ionosphere system, providing valuable insights into the overall dynamics of the system.

The generation of ULF pulsations in the magnetosphere can occur through various mechanisms. The resonant Alfvén wave structures are believed to be one of the major sources, including field line resonances for the shear Alfvén mode from one ionosphere to the conjugate ionosphere and cavity resonances for the fast mode in the

magnetodisk, as well as a lobe resonator in the high Alfvén speed region between the ionosphere and the magnetosphere (Lysak, 2022). Perturbations associated with the radial transport of plasma in the rapidly rotating magnetodisk also play a significant role in driving these waves (Delamere et al., 2015; Khurana et al., 2004; Krupp et al., 2004). Furthermore, internally driven magnetic reconnection in the disk and externally driven events dominated by solar wind also serve as potential sources of ULF pulsations (Dunn et al., 2017; Guo et al., 2018; Kronberg et al., 2012; Yao et al., 2017). It is crucial to consider that large-scale compressions can lead to disturbances within the magnetospheric cavity (Delamere, 2015; Delamere et al., 2014). The external perturbation from the solar wind can also excite ULF waves in the system. For example, Kelvin-Helmholtz instabilities may excite surface waves near the magnetopause propagating into the magnetosphere (Johnson et al., 2014). In order to comprehend the origins of ULF waves and understand the contributions from different sources, it is crucial to explore the distribution of ULF waves in Jupiter's magnetosphere, which can provide important constraints and insights. Manners and Masters (2020) conducted a study on the distribution using data from Pioneer 10 and 11 and Voyager 1 and 2 as well as Ulysses and Galileo. However, due to limitations in data quantity and orbital positions, our understanding of ULF waves concerning different distances and latitudes remains incomplete. In this study, we adopt a unique methodology, utilizing data from the Juno spacecraft, to gain further insights into the distribution of ULF waves and their generation mechanisms within Jupiter's magnetosphere.

In addition to the spatial presence or absence, our inquiry also extends to the periodic characteristics of ULF waves, which is pivotal for delving into their generation mechanisms and analyzing the plasma environment in Jupiter's magnetosphere. Due to the diverse wave excitation mechanisms and the intricate energy propagation processes, the magnetosphere-ionosphere system exhibits a highly dynamic behavior. In the ULF band, ubiquitous quasi-periodic oscillations (QPOs) are widely identified by multiple types of observations, including X-ray, infrared (IR), and ultraviolet (UV) auroral emissions (Dunn et al., 2016; Gladstone et al., 2002; Nichols et al., 2017; Watanabe et al., 2018), magnetic field (Khurana & Kivelson, 1989), radio waves (Arkhypov & Rucker, 2006; Hospodarsky et al., 2004; Kimura et al., 2011, 2012; MacDowall et al., 1993), and energetic particle flux (Karanikola et al., 2004). The phenomena exhibit a wide range of periods typically spanning from 1 to 100 min with a noticeable concentration in the 10–60 min range. There also appear to be several distinct ULF periods, often described as "magic frequencies," around ∼15, ∼30, and ∼40 min (QP-15, QP-30, and QP-40). The presence of similar periods suggests potential correlations and the common underlying physics governing these phenomena.

As one type of QPOs, the auroral emissions indeed provide a visualization of the pulsations in a global context. From 30 November 2016 to 18 July 2017, HST captured a series of ultraviolet (UV) aurora images of Jupiter. Grodent et al. (2018) categorized six aurora morphological classes (Q family, N family, U family, I family, i family, X family) based on the intensity and temporal evolution in the main auroral oval, equatorward and poleward auroras. Moreover, combining coordinated observations by HST and the Juno satellite, Yao et al. (2022) highlighted that the main auroral brightening (MAB) events (corresponding to X family events) arise from magnetospheric compression and are absent under expanded conditions. Similarly, auroral observations in multiple wavelength segments exhibit enhanced brightness (Baron et al., 1996; J. E. P. Connerney & Satoh, 2000; Dunn et al., 2016; Echer et al., 2010; Gurnett et al., 2002; Hess et al., 2014; Nichols et al., 2007, 2009; Sinclair et al., 2019; Zarka & Genova, 1983). In fact, every X-ray observation of Jupiter that is known to have occurred during a solar wind compression at the planet has shown strong periodic pulsations in the X-ray aurora with a characteristic pulsation rate of 9–14 or 24–30 min (Dunn et al., 2016, 2017, 2020; Weigt et al., 2020; Wibisono et al., 2020). Such periodic X-ray pulsations appear to be less prevalent in the aurora during intervals of more quiescent solar wind conditions (Dunn et al., 2020; Wibisono et al., 2021). Yao et al. (2021) show a strong correlation between QPO in the outer magnetosphere magnetic field measurements and X-ray auroral pulsations during July 2017. Although the exact physical mechanism is not yet fully understood, it is clear that solar wind compressions enhance the Jovian auroral emissions globally and across multiple wavebands. What's more, Macdowall et al. (1993) elucidated a correlation between QP radio bursts and the solar wind velocities through data from Ulysses, which intimated the influence of interplanetary conditions. They also emphasized that further examination of the correlations between solar winds and magnetic fields could provide more clues. It would be interesting to explore the potential differences in the occurrence possibility and periodic characteristics of ULF waves in the Jovian magnetosphere under compressed and expanded conditions, which would provide valuable insights into the mechanisms influencing ULF waves and the generation of auroras and QPOs.

On Earth, current systems and Alfvén waves play vital roles in generating auroras. Observation and simulation studies suggest that electromagnetic waves provide driving force for auroral acceleration processes and lead to energy deposition in the ionosphere (Chaston et al., 2005; Keiling et al., 2003, 2019; Lotko et al., 1998). Similarly, on Jupiter, in addition to the corotation breakdown current system (Cowley & Bunce, 2001; Hill, 2001; Southwood & Kivelson, 2001), electromagnetic waves, especially Alfvén waves, have been proposed as an important driver. Observational researches have confirmed the presence of intense Alfvén waves in regions connected to the auroral zone (Saur et al., 2003) and strong Alfvén wave activities at the tail of Io's auroral footprint (Gershman et al., 2019). Furthermore, electron distribution and magnetic perturbations in the auroral region and the magnetosphere also confirmed the importance of Alfvénic acceleration (Lorch et al., 2022; Mauk et al., 2017). Pan et al. (2021) found a strong correlation between the energy of ULF waves with periods ranging from 1 to 60 min and the energy of auroral emissions, particularly in the main aurora. However, further evidence is needed to fully understand the specific mechanisms as well as the contributions of current systems and Alfvén waves to aurora generation. In this study, we further investigate ULF waves in the Jovian magnetosphere and their correlation with auroras, thereby offering new insights into the generation mechanisms of ULF waves and the underlying energy release processes. The subsequent section provides an overview of the data and methodologies employed in this research. In the third section, we present the global distribution of ULF waves in the Jovian magnetosphere using data collected by Juno. Additionally, we explore the interrelationships among magnetospheric compression, auroral brightening and ULF waves through the joint observations of Juno and HST. Finally, we discuss the possible generation mechanisms of ULF waves in Jupiter's magnetosphere based on the statistical results.

2. Data and Methods

This study analyzed magnetic data obtained from the Juno Magnetic Field Investigation (MAG) with 1 s resolution (J. E. P. Connerney et al., 2017). We analyze measurements from 7 July 2016 to 18 August 2022, which cover a distance range of ∼1 R_J to 113 R_J, a local time range of 6LT to 18LT through midnight, and a latitude range from 70°S to 50°N through the equator. The sequential data can then be divided into segments with the length of Jupiter's rotation period. This timescale is appropriate to capture 10-60-min fluctuations around Jupiter during one complete rotation, minimizing potential errors introduced by different locations in the Jupiter-Centered Fixed Coordinate System.

Previous studies on ULF waves typically decompose the magnetic field in the magnetic field-aligned (MFA) coordinate system. However, the data used here exhibit significant variations. The direction of the background field obtained through sliding averaging may have a large angular deviation from the true magnetic field direction, sometimes reaching 180°. Therefore, this study utilizes the total magnetic field data for wave analysis to obtain overall information, while in subsequent case studies, the specific directions of waves can be examined in detail.

We perform the continuous wavelet transform (CWT) on the total magnetic field data. Compared to other spectral methods, the wavelet transform has a better capacity for identifying QPOs (Manners & Masters, 2020). It provides superior simultaneous localization of non-time stationary fluctuations in both frequency and time. The CWT convolves a continuous signal with a set of wavelet basis functions at different scales and time positions to obtain the signal's distribution in the frequency and time domains. Compared to the discrete wavelet transform (DWT), CWT provides higher frequency and time resolution. To address boundary effects in wavelet analysis, we broadened the analysis window to include additional data before and after the target time segment. This strategy ensures the integrity of our analysis of wave fluctuations within the designated timeframe, avoiding distortions due to edge artifacts. We calculate the wavelet power spectral density (PSD), providing a time-frequency representation of magnetic field fluctuations. By performing a time integration, the time-average wavelet PSD distribution across frequencies can be obtained within each time window. The peaks in this distribution mark the quasi-periodic phenomena of interest. It should be noted that whenever we are talking about a period in this study, we actually mean a quasi-period, since it is not a strictly periodic signal that is recorded. By statistically analyzing these periodic peaks, we provide global characteristics of QPOs in Jupiter's magnetosphere. Figure 1 shows an example application of this process and the detection of QPO signatures in the magnetic field data. The significance levels were calculated employing the approach described in Torrence and Compo (1998).

Furthermore, this study also combines auroral observations from the HST program GO-14634 conducted with the Space Telescope Imaging Spectrograph (STIS) ultraviolet camera. The program coincides with Juno orbits 3–7,

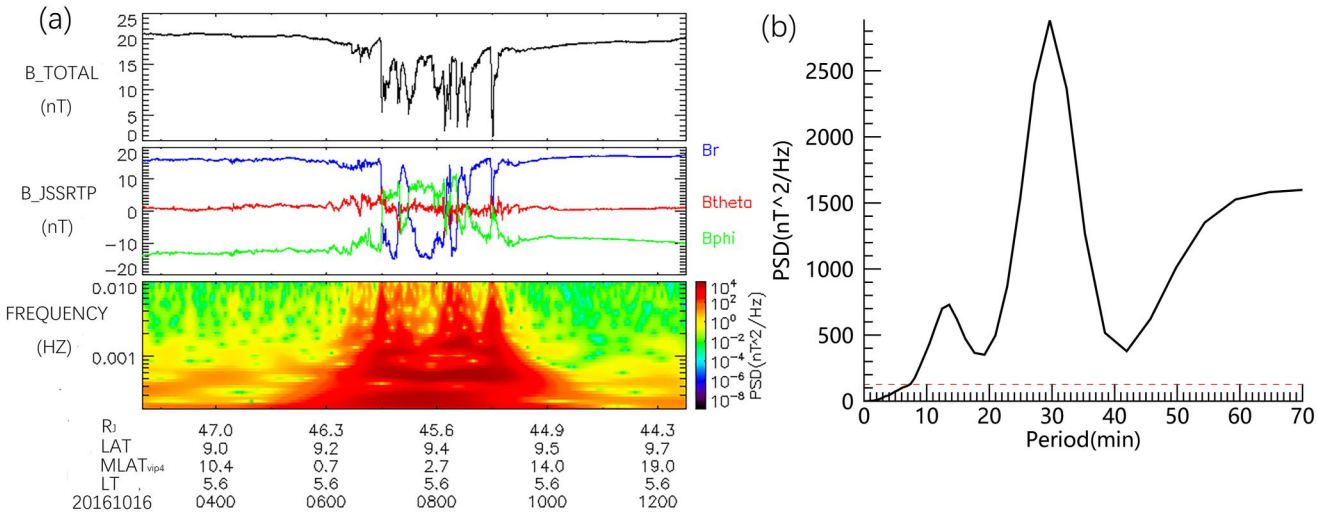

Figure 1. Analysis framework showing magnetometer data from the Juno spacecraft during 2:40–12:30 on 16 October 2016. (a) From top to bottom: the total magnetic field, r-theta-phi magnetic field components in Jupiter-de-Spun-Sun (JSS) coordinate, and the power spectral density (PSD) obtained by wavelet analysis. (b) The time-average wavelet PSD distribution across frequencies. The red dashed line represents the 99% significance level computed according to Torrence and Compo (1998).

providing a good opportunity for contemporaneous comparison of Jupiter's auroras with the state of the magnetosphere. Given the absence of real-time observations of solar wind conditions at Jupiter, we adopted auroral observations to estimate the level of magnetospheric compression. Our statistical study is based on the list of auroral characteristics derived by Grodent et al. (2018), and mainly focuses on the X and Q family auroras, which are considered to correspond to the compressed and the quiet magnetospheres, respectively, in Yao et al. (2022) and Grodent et al. (2018).

3. Results

We analyzed the total magnetic field data and collected the periodic peaks, showing the distributions of periods in different regions in Figure 2. The period range from 2.5 to 72.5 min was divided into 14 intervals of 5 min each. We count the number of events showing periodic peaks of each interval in different distance ranges (30–50 R_J, 50–70 R_J, 70–90 R_J, and 90–110 R_J) for both low latitudes (0–10°, represented by green) and mid latitudes (20°–40°, represented by yellow) in Jupiter's planetocentric system. The statistical results were then normalized to the total number of time segments satisfying the corresponding spatial conditions, so that the relative heights of the bars indicate the occurrence probability of different quasi-periods in the described region. We categorized the total number of observation events under different distance and latitude conditions as follows: (a) 30–50 R_J: 134 (low latitude), 154 (middle latitude); (b) 50–70 R_J: 158 (low latitude), 314 (middle latitude); (c) 70–90 R_J: 189 (low latitude), 566 (middle latitude); (d) 90–110 R_J: 542 (low latitude), 1351 (middle latitude). Since some intervals do not exhibit period peaks and others show single or multiple peaks, the sum of occurrence rates may not equal 1.

Periods span the full 5–70 min range in particular the 10–60 min range reported in the literature. In the low-latitude magnetosphere, the probability of occurrence of ULF waves appears to be largely independent of distance. There is a suggestion of peaks consistent with the "magic frequencies" QP-15, QP-30, and QP-40. The QP-15 and QP-30 appear to be widely distributed over 10–30 min range rather than two discrete peaks. Regarding the mid-latitude magnetosphere, ULF waves are increasingly obvious from 50 R_J to 110 R_J, and almost no fluctuations can be observed within 30–50 R_J. This could be attributed to the fact that for the mid-latitude magnetosphere, being farther out implies closer proximity to the magnetopause, resulting in more disturbance events due to fluctuations near the magnetopause. Compared with low-latitude regions, the 10–30 min periods in mid-latitude regions are not always prominent, but there is a peak at 25 min. The 40 min peak can also be vaguely distinguished, and this region exhibits relatively evenly distributed 45–70 min periods similar to the low latitude. Overall, latitude appears to have a more pronounced impact on the distribution of ULF waves compared with distance. The low-latitude regions are more abundant with waves with periods of 40 min or shorter, which may indicate an extra and independent source in the magnetodisk.

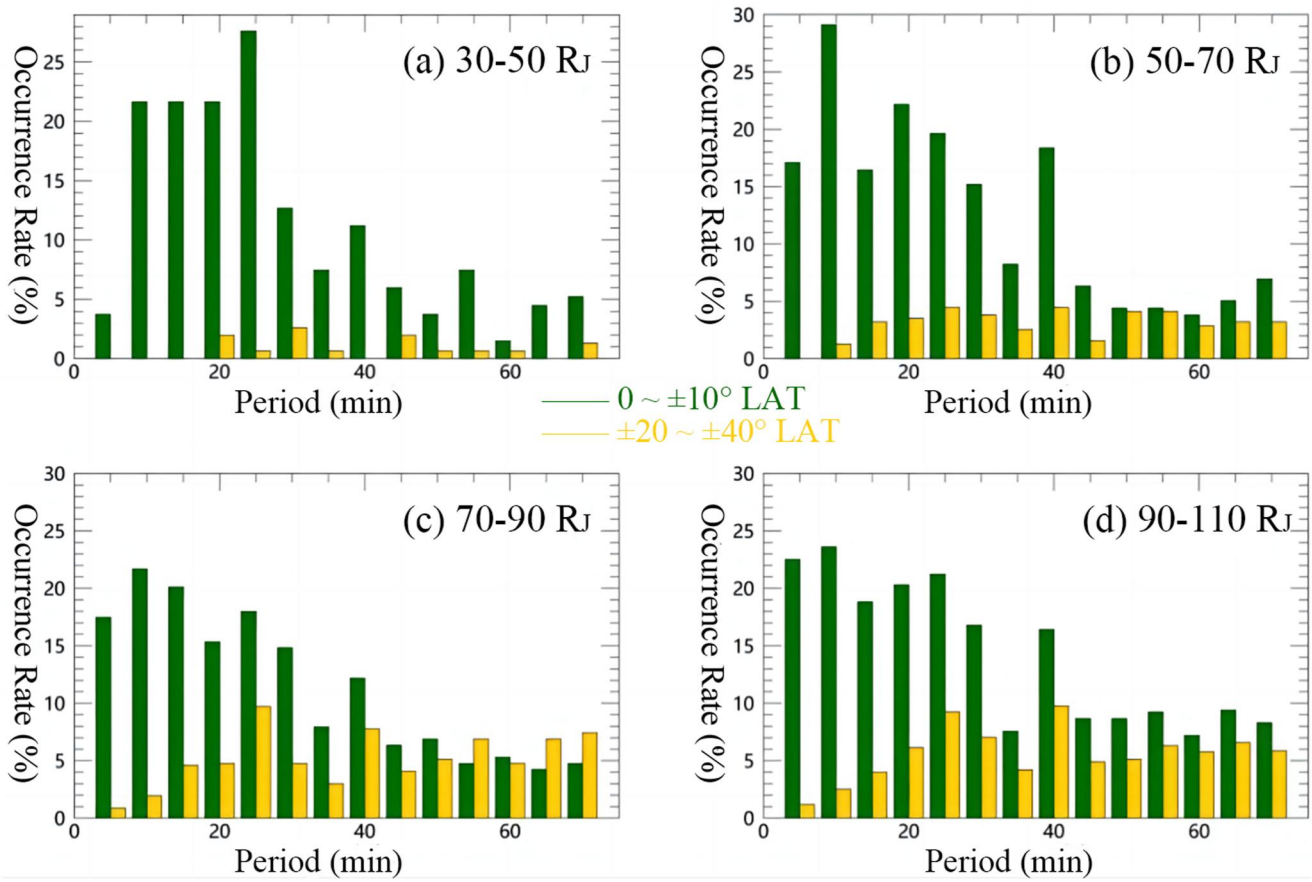

Figure 2. Normalized histograms of significant periods in four distance sectors: (a) 30–50 R_J, (b) 50–70 R_J, (c) 70–90 R_J, and (d) 90–110 R_J. The green and yellow columns correspond to the low (0–10°) and middle (20–40°) latitude regions, respectively. The latitude seems to play a more important role than the distance.

In order to investigate the possible superposition of multiple source mechanisms and possible harmonic phenomena, we obtained the distribution of single-period and multi-period (10–60 min) events in Figure 3a, while Figure 3b displays the ratio of multi-period events to all observed ULF wave events across different regions. From dawnside to nightside to duskside, the inclination of the Juno orbits gradually increased. Observing the green-dominated dawnside and the red-dominated duskside in Figure 3a, as well as the color distribution in Figure 3b, it is evident that the proportion of multi-period wave events in the low-latitude regions far exceeds that in the mid-latitude areas, with a discrepancy reaching 50%. These results provide constraints and indications for discerning the sources of ULF waves in the magnetosphere. For the duskside of middle latitudes, the disturbance might mainly come from the magnetopause. The high proportion of multi-peak events in the low-latitude regions on the nightside suggests the potential coexistence of multiple ULF wave driving mechanisms within the magnetodisk. The dawnside of low latitudes may be influenced by both the magnetopause and the dynamic processes in the magnetodisk. Additionally, the multi-period phenomenon could also be derived from harmonic structures (Manners & Masters, 2019), especially when the present multiple periods are proportional.

In addition to the spatial distribution of ULF waves, the factors influencing their temporal variation are also important in understanding the Jovian system energy processes. Here, we mainly discuss the differences between compression and expansion conditions identified by HST observations. In the comparison of HST-Juno simultaneous observations, time correction needs to be carefully considered. First, due to the distance between Earth and Jupiter, there is a time delay from the occurrence of auroras to the observation by the telescope. At the same time, the duration of X- or Q-family auroras is, in fact, not confined solely to the HST observation time, but may extend over several hours both preceding and following the observation. In addition, it is worth noting that different events correspond to different positions of Juno in the magnetic coordinate system. The Juno was sometimes in the magnetodisk during HST's exposure, and sometimes it was not. This may introduce potential

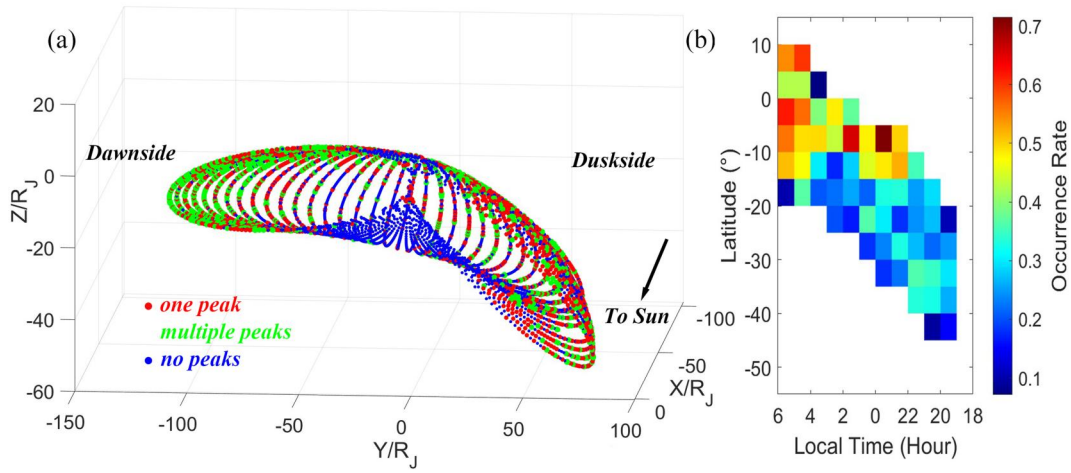

Figure 3. The spatial distribution of quasi-periodic magnetic field fluctuations (10–60 min). (a) A 3-D plot in the JSS coordinate system. The red, green, and blue dots represent cases with one periodic peak, multiple peaks and no peaks on timescales of 10–60 min, respectively. (b) The ratio of multi-peak events to total ULF wave events in each region. The local time is plotted on the *x*-axis, while the latitude is shown on the *y*-axis. White areas represent regions with fewer than 10 ULF wave events.

issues in our comparative analysis. To ensure comparability and involve the observations of the closest current sheet crossings, we chose to analyze the data during a period spanning several hours before and after the corrected Juno time when HST acquired the images.

The two tables provide the times when the auroral morphology was either in the Q family or the X family, respectively. Both tables display the auroral brightness, the positions of Juno, and the corresponding magnetic field wave characteristics. It can be observed that regardless of the extended time windows of 3, 6, or 10 hr (1.5, 3, or 5 hr before and after the telescope shot), the X family auroras consistently correspond to distinct quasi-periodic peaks, often showing multiple periods. On the other hand, the Q family auroras seldom occur with such quasi-periodicity, and no multi-periodic behavior has been observed. We conducted 100,000 random samplings of our database, wherein nine instances were labeled as fake X events and 11 instances were labeled as fake Q events in each iteration. The analysis revealed that the frequency of observing such imbalances randomly was found to be only 0.03%. Additionally, the chi-square test shows that there is 99.7% certainty that the occurrence possibility of ULF waves is related to the auroral family (the magnetospheric state). Figure 4 respectively gives examples of magnetic field features of X and Q-family events, between which we can see a clear contrast. During the corresponding interval of X-family auroras, magnetic field disturbances were more pronounced, whereas the magnetic field during Q-family auroras remained relatively quiet. In these two 10-hr intervals, the Juno satellite was at roughly similar locations, at a distance of 76–79 R_J, a latitude of about ±0.6°, and a local time of 4.5–4.9 LT. The similarity in location makes the temporal variations brought about by different magnetospheric states more explicit.

We display the distribution of periodic peaks obtained in 10-hr time windows in Figure 5. The periods of ULF waves during X-family auroras are clustered in the 10–30 min range. As for Q family, it is challenging to observe the distribution due to the scarcity of periodic peaks, but they seem to exhibit a higher occurrence rate in periods above 30 min compared to X-family events. In summary, this comparison suggests the different ULF wave features in the compressed and calm magnetosphere (corresponding to the X and Q auroras) from Tables 1 and 2 and Figures 4 and 5, although we note the limited data set and possible randomness.

4. Discussion

In this study, we utilize data gathered during 6 years by the MAG instrument onboard the Juno spacecraft to perform a statistical analysis of ULF waves in Jupiter's magnetosphere. This research marks the first time such an analysis has been performed using these specific instruments. Our investigation focuses on the global distribution of ULF waves and their periodic characteristics across various regions of the Jovian magnetosphere.

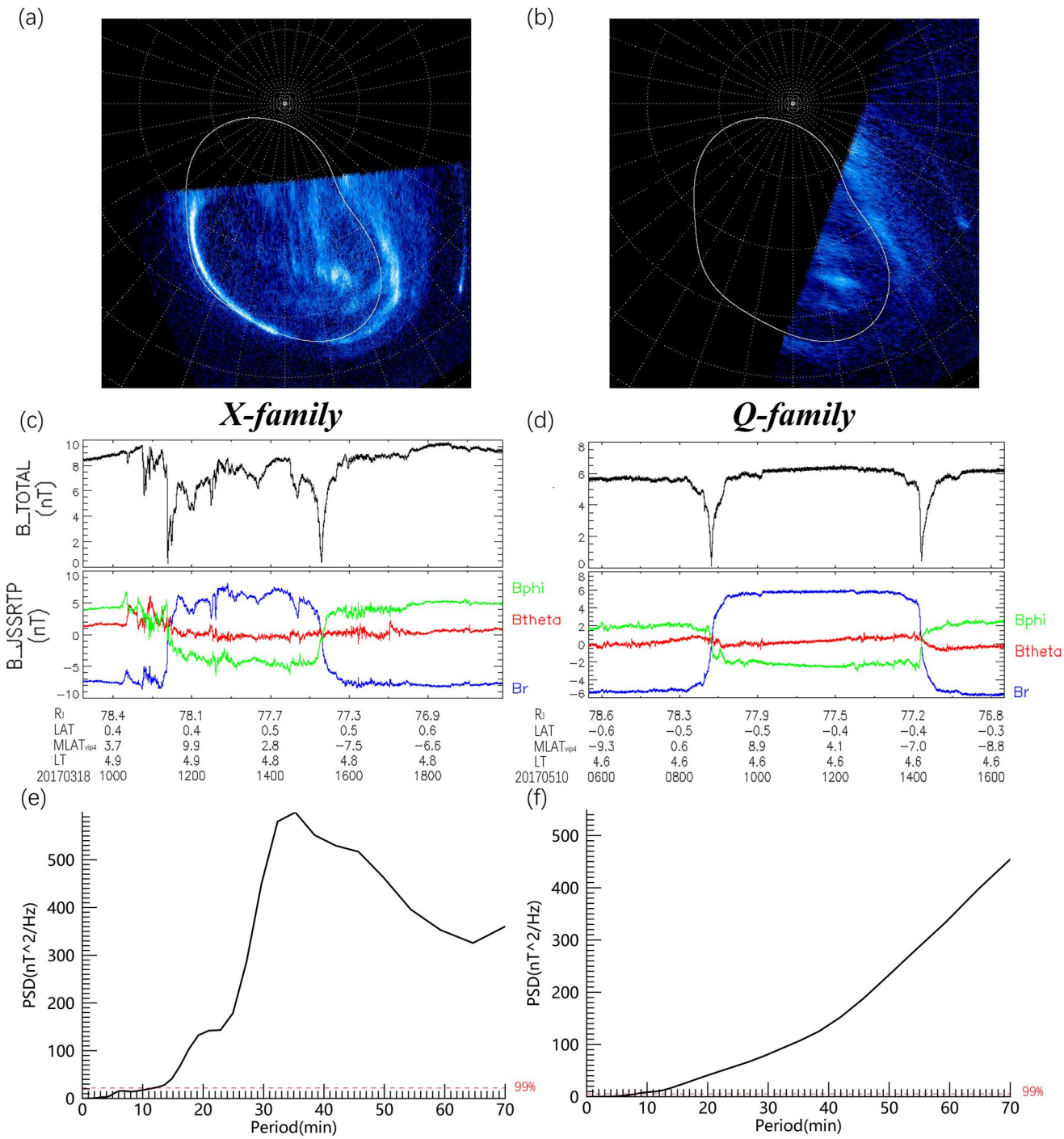

Figure 4. Two examples showing magnetic field features in 10-hr window of X-family (od8k42fiq observation, see Table 1) and Q-family (od8k62ogq observation, see Table 2) events, presented in (a, c, e) and (b, d, f), respectively. (a, b) Two auroral images acquired by HST. (c, d) From top to bottom: the total magnetic field and r-theta-phi magnetic field components in JSS coordinate. (e, f) The time-average wavelet PSD distribution across frequencies. The red dashed line represents the 99% significance level.

The distribution of ULF waves is a consequence of the combined influence of both internal and external driving mechanisms. It is widely accepted that under the influence of centrifugal forces, the Rayleigh-Taylor instability facilitates the outward transport of plasma, a process achieved through the interchange of magnetic flux tubes. In the magnetospheric context of rapidly rotating systems, such as Jupiter, the magnetic curvature forces often dominate over centrifugal forces (Southwood & Kivelson, 1987). Simulation-based investigations show that the

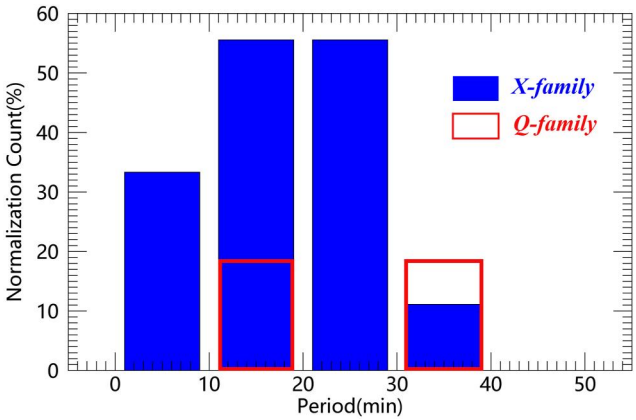

Figure 5. The distribution of periods identified in 10-hr windows corresponding to the Q-family (red box) and X-family (solid blue square) auroras, normalized according to the total number of selected events (11 for Q and 9 for X).

magnetodisk of Jupiter contains multiple finger-like interchange structures (Feng et al., 2023; Schok et al., 2023). These structures, influenced by planetary rotation modulation, may produce periodic perturbations in in situ measurements and result in an additional ULF wave source. The periodicity arising from these interchange structures is determined by their wave number, which may vary from several to tens, corresponding to periods of 10–60 min. Such interchange structures are also dynamically evolving. According to the analysis of quasi-interchange mode in giant planet magnetospheres by Achilleos et al. (2015), the condition of the generalized Rayleigh-Taylor frequency squared $\omega_0^2 \geq 0$ is necessary and sufficient for the stability of the interchange mode.

$$\omega_0^2 = \left(\frac{\nabla\rho}{\rho} - 2\mathbf{c}\right)\cdot\mathbf{g} + \left[\frac{\nabla(2P_M + P_\perp - P_\parallel)}{\rho} - \left(V_A^2 + C_\perp^2 - 4C_\parallel^2\right)\mathbf{c}\right]\cdot\mathbf{c} - \frac{\left[\mathbf{g} + \left(V_A^2 - C_\parallel^2\right)\mathbf{c}\right]^2}{V_A^2 + 2C_\perp^2}.$$

Here, ρ denotes the plasma mass density, g the effective gravity (including a centrifugal component) with unit vector $\hat{e_g} = g/g, c$ the magnetic curvature vector, $C_\perp^2 = (P_\perp/\rho)$, $C_\parallel^2 = (P_\parallel/\rho)$ where the corresponding plasma pressures are $P_\perp$ (perpendicular to the magnetic field) and $P_\parallel$ (parallel to the magnetic field). P_M denotes magnetic pressure. It also involves the Alfvén speed, V_A, and sound speeds in directions perpendicular and parallel to the magnetic field (respectively $C_\perp$ and $C_\parallel$). When Jupiter's magnetosphere is compressed by the solar wind pressure, the current sheet becomes thinner (Xu et al., 2023), leading to an increase in magnetic field curvature (c) (Rogers et al., 2023). As a result, ω_0^2 is more likely to fall below 0, which conveys the growth of interchange instability and gives rise to more prominent structures for transporting plasma outward. Conversely, when the current sheet is relatively thick, interchange structures are less likely to emerge within the magnetodisk, leading to a reduced likelihood of observing quasi-periodic phenomena. Theoretical predictions align with observational evidence. In this study, we have observed more distinct ULF waves in the low-latitude magnetodisk during X-family auroral events corresponding to compressed conditions, whereas they were not as pronounced during Q-family auroral events.

Table 1
Quasi-Periodic Fluctuations During the X-Family Auroras

Rootname	Date (dd/mm/yyyy)	Time (hh:mm:ss)	Auroral brightness/TW	Distance/R_J	Latitude/°	Local time	Period (~3-hr window)/min	Period (~6-hr window)/min	Period (~10-hr window)/min
od8k01r0q	11/30/2016	14:57:23	1.5872	87.0	0.96	5.40	16, 35, 54	14, 30	14, 30
od8k02r4q	11/30/2016	16:32:45	1.40442	86.8	1.00	5.40	12, 54	14	14, 30
od8k05vnq	12/01/2016	16:23:32	1.7525	82.9	1.57	5.39	10, 23, 59	25	25
od8k11fuq	12/05/2016	18:56:58	1.65873	62.8	4.84	5.37	23	6, 21	10, 21
od8k12j9q	12/06/2016	14:02:21	1.98114	57.9	5.76	5.37	16	16	16
od8k32anq	03/17/2017	8:01:34	2.46697	82.9	−0.32	4.86	25	27	27
od8k42fiq	03/18/2017	14:14:38	2.08424	77.6	0.5	4.85	21, 46	46	35
od8k57itq	03/19/2017	9:19:18	2.59752	73.9	1.1	4.84	10	9, 16	10, 16
od8k69idq	06/18/2017	9:13:04	2.07849	111.1	−7.54	4.4	19	19	8, 19

Note. The first four columns of the table provide the HST archive root name, the corresponding time at Juno corrected for light travel time at the start of the exposure (dd/mm/yyyy hh:mm:ss format) and auroral brightness from Grodent et al. (2018). Subsequently, we present Juno's distance, latitude, local time, and the quasi-periods of the magnetic field within 3 hr (approximately 1.5 hr before and after), 6 hr (approximately 3 hr before and after), and 10 hr (approximately 5 hr before and after) centered around the exposure time. We exclude an X-family event from Grodent et al. (2018) due to significant differences in Juno's location, making it difficult to compare with the statistics above and other events.

Table 2
Quasi-Periodic Fluctuations During the Q-Family Auroras

Rootname	Date (dd/mm/yyyy)	Time (hh:mm:ss)	Auroral brightness/TW	Distance/R_J	Latitude/°	Local time	Period (~3-hr window)/min	Period (~6-hr window)/min	Period (~10-hr window)/min
od8k26q4q	12/04/2016	12:44:51	0.99415	70.0	3.63	5.38	19	19	19
od8k15qdq	12/13/2016	11:21:37	0.702831	30.2	−24.4	5.34	None	None	None
od8k16yrq	12/15/2016	7:50:44	0.919639	47.2	−19.1	5.33	None	None	None
od8k63neq	05/10/2017	5:54:33	0.776101	78.6	−0.58	4.58	None	None	None
od8k62ogq	05/10/2017	10:40:39	1.00931	77.7	−0.45	4.58	None	None	None
od8k84c6q	05/13/2017	8:36:44	1.16827	62.6	2.03	4.56	None	None	None
od8k87d1q	05/15/2017	11:28:13	0.902056	48.3	4.93	4.55	None	None	None
od8k0qldq	07/05/2017	8:05:37	0.936805	61.7	1.25	4.29	32	32	32
od8k0eqaq	07/06/2017	23:49:38	1.14375	50.7	3.46	4.28	11	None	16
od8k0twqq	07/08/2017	4:28:27	0.936659	41.0	5.84	4.27	None	32	None
od8k0fwuq	07/08/2017	6:01:24	0.923965	40.5	6.00	4.27	32	35	38

Note. The format is the same as in Table 1. We exclude two Q-family events from Grodent et al. (2018).

The internal sources of ULF waves include field line resonances, cavity resonances, and magnetic reconnection, while the external sources include solar wind dynamic pressure impulses and Kelvin-Helmholtz instability. These mechanisms can occur both independently and interactively, collectively influencing the excitation and characteristics of ULF waves. As discussed in Figure 3, the low-latitude magnetosphere appears to be influenced by two or more driving sources, while the mid-latitude magnetosphere is likely primarily affected by external driving factors. From this perspective, it can be conjectured that under the influence of external driving, ULF waves predominantly exhibit periodicities around 25 and 40 min in the mid-latitude regions. ULF waves primarily manifest periodicities ranging from 5 to 40 min under internal driving.

The results of the statistical research in this paper enhance our understanding of the excitation of ULF waves through field line resonances and cavity resonances within Jupiter's plasma environment. Lysak and Song (2020) employed the magnetic field model developed by J. E. P. Connerney et al. (1981) and the plasma model by Bagenal and Delamere (2011) to perform time-domain simulations of Alfvén waves propagating along Jovian magnetic field lines. They found that the model could support a diverse range of frequencies, particularly in the 10–40 min range. These findings align with our statistical results, revealing a prevalence of waves in the 10–40 min range and lower occurrence rates in the 45–70 min range within the low-latitude magnetosphere. It is likely that this phenomenon arises from the combined effects of field line resonances and cavity resonances coupling in the magnetodisk. Certain regions with specific magnetic field strengths or topologies could exert inhibitory effects on waves within the 45–70 min range. Furthermore, such wave distributions are widely spread in the region of 30–110 R_J, indicating their presence throughout a substantial portion of Jupiter's magnetosphere. As posited by Lysak (2022), the Jovian tail is more conducive to supporting field line resonances at larger radial distances from the planet compared to Earth. Our statistical findings lend support to the extension of the range of field line resonances within Jupiter's magnetosphere beyond 100 R_J.

Magnetic reconnection is also considered a potential internal trigger source for ULF waves. Recent research by Vogt et al. (2020) has highlighted the widespread occurrence of magnetic reconnection in Jupiter's magnetotail. We also noticed that the majority of X-type auroral events appear to be potentially associated with events listed in their magnetic reconnection catalog. Moreover, reconnection events at the magnetopause have also been invoked to account for the observed quasi-periodic phenomena. By analogy with Earth, Bunce et al. (2004) estimated that the reconnection interpulse period at Jupiter could be around 30–50 min, which may provide a plausible explanation of the pulsed X-ray emissions and the 40-min peak observed in this study. These findings suggest that magnetic reconnection plays a significant role in the generation of ULF waves in Jupiter's magnetosphere. However, further research is required to fully understand the specific mechanisms and dynamics involved in this process.

In addition to internal triggering mechanisms such as field line resonances, cavity resonances and magnetic reconnection, external driving can also impact wave generation. The increased occurrence rates under magnetospheric compression conditions and the distance-dependent distribution of ULF waves in mid-latitude regions observed on Jupiter appear to be related to external driving factors. The Kelvin-Helmholtz instability (KHI) and solar wind dynamic pressure impulses are acknowledged as two primary external sources believed to stimulate wave excitation (Zong et al., 2017). Evidence of KHI-driven waves along Jupiter's dawn flank magnetopause during the Juno prime mission (Montgomery et al., 2023). Simulation results indicate that the period of density fluctuations at the dusk terminator flank (18 magnetic local time, MLT) is approximately 1.4 hr (Zhang et al., 2018). The second harmonic (42 min) and the third harmonic (28 min) may account for the observed peaks at 40 and 25 min in the mid-latitude magnetosphere. Further research is needed to fully understand the specific mechanisms and dynamics involved in this process.

Internal and external driving mechanisms can account for the relationship between the occurrence rate of ULF waves and magnetospheric compression conditions. One scenario posits that magnetospheric compression leads to the generation of compression waves, while interactions with the solar wind induce magnetopause K-H instability, resulting in quasi-periodic fluctuations with periods of around 25 and 40 min. For another, the increased proximity of magnetic field lines facilitates the occurrence of magnetic reconnection events in the magnetotail, generating ULF waves with periods of 5–30 min. Notably, the observed periods during X-family auroras predominantly fall within the 5–30 min range, which seems to provide some additional support for the dominance of the latter mechanism.

Our findings resonate with the observations made by Macdowall et al. (1993), suggesting that solar wind conditions have a significant impact on the occurrence rate of quasi-periodic radio bursts and magnetic field fluctuations.

We also pay attention to the relationship between ULF waves and aurorae. Under compressed conditions, ULF waves with periods concentrated in the 10–30 min range exhibit consistency with the 9–14 or 24–30 min periods in the X-ray observations mentioned in the Introduction. Under quiet magnetospheric conditions, the low occurrence rate of ULF waves in this statistical analysis also aligns with the absence of observed X-ray auroral pulsations. This adds new information to the elucidation of the correlation between ULF waves and auroras. It is also comprehensible that certain time intervals corresponding to Q-family auroras display periodic peaks. Jupiter's magnetosphere is a highly intricate and dynamic system; thus, the continuous presence of ULF waves is expected, though their quantity and intensity may occasionally be diminished. Additionally, it is important to note that within the chosen 3–10-hr time intervals, the magnetospheric state may have undergone significant changes, such as transitioning from a quiet state to a more active one. Therefore, the aurora observed by HST may not fully represent the actual magnetospheric state.

5. Conclusion

This study provides a global perspective on the spatial distribution, periodic characteristics and potential sources of ULF waves within Jupiter's magnetosphere, contributing to a deeper understanding of the energy releases on timescales of 10–60 min. The main results are summarized as follows:

1. In the analysis of the spatial distribution and periodic features of ULF waves, it becomes evident that latitude plays a more substantial role than distance. The occurrence rate of ULF waves is observed to be higher in low-latitude regions and remains relatively constant with distance. In mid-latitude regions, the occurrence rate is relatively lower but displays a slight increase at greater distances.
2. In the mid-latitude region, a similar QP-40 and 45–70 min period distribution structure as that in the low-latitude region is observed. Additionally, another distribution peak is observed at approximately 25 min, which is also present in the low-latitude region where ULF waves in the 10–30 min range are abundant.
3. It has been consistently observed that ULF waves are present during episodes of enhanced X-family auroras that are associated with magnetospheric compression. However, this phenomenon is not evident during Q-family auroras, which correspond to quiet conditions.
4. The observed quasi-periodic magnetic field fluctuations are likely attributed to the interchange structures within the Jupiter's magnetodisc, as well as field line resonances and cavity resonances possibly triggered by concurrent processes such as magnetic reconnection and the Kelvin-Helmholtz instability.

In future studies, the combination of periods of quasi-periodic phenomena in multiple data sets (including magnetic fields, particles, auroras, etc.) may provide more evidence to reveal dynamic processes in Jupiter's magnetosphere. In the meantime, we will select typical cases for comprehensive in-depth analysis of ULF wave characteristics, hoping to be able to build a more complete picture of the energy transfer and release in Jupiter's magnetosphere.

Data Availability Statement

The Juno data presented in this study are available at http://pds-ppi.igpp.ucla.edu/ via the MAG instrument (J. Connerney, 2022). The auroral images are based on observations with the NASA/ESA HST (program HST GO-14634) obtained at the Space Telescope Science Institute (STScI), which is operated by AURA for NASA. These data are publicly available at STScI via https://archive.stsci.edu/hst/. The auroral list used is available at https://doi.org/10.1002/2017JA025046 (Grodent et al., 2018).

Acknowledgments
Z. Y. acknowledges the National Science Foundation of China (Grant 42074211). WRD is supported by STFC Ernest Rutherford Fellowship ST/W003449/1. Wavelet software was provided by C. Torrence and G. Compo, and is available at URL: http://paos.colorado.edu/research/wavelets/.

References

Achilleos, N., André, N., Blanco-Cano, X., Brandt, P. C., Delamere, P. A., & Winglee, R. (2015). 1. Transport of mass, momentum and energy in planetary magnetodisc regions. *Space Science Reviews*, *187*(1–4), 229–299. https://doi.org/10.1007/s11214-014-0086-y

Arkhypov, O., & Rucker, H. (2006). Ultra low frequencies phenomena in Jovian decametric radio emission. *Astronomy & Astrophysics*, *452*(1), 347–350. https://doi.org/10.1051/0004-6361:20054334

Bagenal, F., & Delamere, P. A. (2011). Flow of mass and energy in the magnetospheres of Jupiter and Saturn: Mass and energy. *Journal of Geophysical Research*, *116*(A5). https://doi.org/10.1029/2010JA016294

Bagenal, F., Wilson, R. J., Siler, S., Paterson, W. R., & Kurth, W. S. (2016). Survey of Galileo plasma observations in Jupiter's plasma sheet. *Journal of Geophysical Research: Planets*, *121*(5), 871–894. https://doi.org/10.1002/2016JE005009

Baron, R. L., Owen, T., Connerney, J. E. P., Satoh, T., & Harrington, J. (1996). Solar wind control of Jupiter's H^+_3Auroras. *Icarus*, *120*(2), 437–442. https://doi.org/10.1006/icar.1996.0063

Bunce, E. J., Cowley, S. W. H., & Yeoman, T. K. (2004). Jovian cusp processes: Implications for the polar aurora. *Journal of Geophysical Research*, *109*(A9), 2003JA010280. https://doi.org/10.1029/2003JA010280

Chaston, C. C., Peticolas, L. M., Carlson, C. W., McFadden, J. P., Mozer, F., Wilber, M., et al. (2005). Energy deposition by Alfvén waves into the dayside auroral oval: Cluster and FAST observations. *Journal of Geophysical Research*, *110*(A2). https://doi.org/10.1029/2004JA010483

Connerney, J. (2022). Juno magnetometer Jupiter archive JNO-J-3-FGM-CAL-V1.0 [Dataset]. NASA Planetary Data System. https://doi.org/10.17189/1519711

Connerney, J. E. P., Acuña, M. H., & Ness, N. F. (1981). Modeling the Jovian current sheet and inner magnetosphere. *Journal of Geophysical Research*, *86*(A10), 8370–8384. https://doi.org/10.1029/JA086iA10p08370

Connerney, J. E. P., Benn, M., Bjarno, J. B., Denver, T., Espley, J., Jorgensen, J. L., et al. (2017). The Juno magnetic field investigation. *Space Science Reviews*, *213*(1–4), 39–138. https://doi.org/10.1007/s11214-017-0334-z

Connerney, J. E. P., & Satoh, T. (2000). The H^+_3 ion: A remote diagnostic of the Jovian magnetosphere. *Philosophical Transactions of the Royal Society B: Biological Sciences*, *358*(1774), 2471–2483. https://doi.org/10.1098/rsta.2000.0661

Cowley, S. W. H., & Bunce, E. J. (2001). Origin of the main auroral oval in Jupiter's coupled magnetosphere–ionosphere system. *Planetary and Space Science*, *49*(10), 1067–1088. https://doi.org/10.1016/S0032-0633(00)00167-7

Delamere, P. A. (2015). Solar wind interaction with giant magnetospheres and Earth's magnetosphere. In *Magnetotails in the solar system* (pp. 217–233). American Geophysical Union (AGU). https://doi.org/10.1002/9781118842324.ch13

Delamere, P. A., Bagenal, F., Paranicas, C., Masters, A., Radioti, A., Bonfond, B., et al. (2014). Solar wind and internally driven dynamics: Influences on magnetodiscs and auroral responses. *Space Science Reviews*, *187*(1), 51–97. https://doi.org/10.1007/s11214-014-0075-1

Delamere, P. A., Otto, A., Ma, X., Bagenal, F., & Wilson, R. J. (2015). Magnetic flux circulation in the rotationally driven giant magnetospheres. *Journal of Geophysical Research: Space Physics*, *120*(6), 4229–4245. https://doi.org/10.1002/2015JA021036

Dunn, W. R., Branduardi-Raymont, G., Elsner, R. F., Vogt, M. F., Lamy, L., Ford, P. G., et al. (2016). The impact of an ICME on the Jovian X-ray aurora. *Journal of Geophysical Research: Space Physics*, *121*(3), 2274–2307. https://doi.org/10.1002/2015JA021888

Dunn, W. R., Branduardi-Raymont, G., Ray, L. C., Jackman, C. M., Kraft, R. P., Elsner, R. F., et al. (2017). The independent pulsations of Jupiter's northern and southern X-ray auroras. *Nature Astronomy*, *1*(11), 758–764. https://doi.org/10.1038/s41550-017-0262-6

Dunn, W. R., Gray, R., Wibisono, A. D., Lamy, L., Louis, C., Badman, S. V., et al. (2020). Comparisons between Jupiter's X-ray, UV and radio emissions and in-situ solar wind measurements during 2007. *Journal of Geophysical Research: Space Physics*, *125*(6), e2019JA027222. https://doi.org/10.1029/2019ja027222

Echer, E., Zarka, P., Gonzalez, W., Morioka, A., & Denis, L. (2010). Solar wind effects on Jupiter non-Io DAM emissions during Ulysses distant encounter (2003-2004). *Astronomy & Astrophysics*, *519*, A84. https://doi.org/10.1051/0004-6361/200913305

Feng, E., Zhang, B., Yao, Z., Delamere, P. A., Zheng, Z., Dunn, W. R., & Ye, S. (2023). Variation of the Jovian magnetopause under constant solar wind conditions: Significance of magnetodisc dynamics. *Geophysical Research Letters*, *50*(12), e2023GL104046. https://doi.org/10.1029/2023GL104046

Gershman, D. J., Connerney, J. E. P., Kotsiaros, S., DiBraccio, G. A., Martos, Y. M., Viñas, A. F., et al. (2019). Alfvénic fluctuations associated with Jupiter's auroral emissions. *Geophysical Research Letters*, *46*(13), 7157–7165. https://doi.org/10.1029/2019GL082951

Gladstone, G. R., Waite, J. H., Grodent, D., Lewis, W. S., Crary, F. J., Elsner, R. F., et al. (2002). A pulsating auroral X-ray hot spot on Jupiter. *Nature*, *415*(6875), 1000–1003. https://doi.org/10.1038/4151000a

Grodent, D., Bonfond, B., Yao, Z., Gérard, J.-C., Radioti, A., Dumont, M., et al. (2018). Jupiter's aurora observed with HST during Juno orbits 3 to 7. *Journal of Geophysical Research: Space Physics*, *123*(5), 3299–3319. https://doi.org/10.1002/2017JA025046

Guo, R. L., Yao, Z. H., Wei, Y., Ray, L. C., Rae, I. J., Arridge, C. S., et al. (2018). Rotationally driven magnetic reconnection in Saturn's dayside. *Nature Astronomy*, *2*(8), 640–645. https://doi.org/10.1038/s41550-018-0461-9

Gurnett, D. A., Kurth, W. S., Hospodarsky, G. B., Persoon, A. M., Zarka, P., Lecacheux, A., et al. (2002). Control of Jupiter's radio emission and aurorae by the solar wind. *Nature*, *415*(6875), 985–987. https://doi.org/10.1038/415985a

Hess, S. L. G., Echer, E., Zarka, P., Lamy, L., & Delamere, P. A. (2014). Multi-instrument study of the Jovian radio emissions triggered by solar wind shocks and inferred magnetospheric subcorotation rates. *Planetary and Space Science*, *99*, 136–148. https://doi.org/10.1016/j.pss.2014.05.015

Hill, T. W. (2001). The Jovian auroral oval. *Journal of Geophysical Research*, *106*(A5), 8101–8107. https://doi.org/10.1029/2000JA000302

Hospodarsky, G. B., Kurth, W. S., Cecconi, B., Gurnett, D. A., Kaiser, M. L., Desch, M. D., & Zarka, P. (2004). Simultaneous observations of Jovian quasi-periodic radio emissions by the Galileo and Cassini spacecraft. *Journal of Geophysical Research*, *109*(A9). https://doi.org/10.1029/2003JA010263

Johnson, J. R., Wing, S., & Delamere, P. A. (2014). Kelvin Helmholtz instability in planetary magnetospheres. *Space Science Reviews*, *184*(1), 1–31. https://doi.org/10.1007/s11214-014-0085-z

Karanikola, I., Athanasiou, M., Anagnostopoulos, G. C., Pavlos, G. P., & Preka-Papadema, P. (2004). Quasi-periodic emissions (15–80 min) from the poles of Jupiter as a principal source of the large-scale high-latitude magnetopause boundary layer of energetic particle. *Planetary and Space Science*, *52*(5), 543–559. https://doi.org/10.1016/j.pss.2003.10.002

Keiling, A., Thaller, S., Wygant, J., & Dombeck, J. (2019). Assessing the global Alfvén wave power flow into and out of the auroral acceleration region during geomagnetic storms. *Science Advances*, *5*(6), eaav8411. https://doi.org/10.1126/sciadv.aav8411

Keiling, A., Wygant, J. R., Cattell, C. A., Mozer, F. S., & Russell, C. T. (2003). The global morphology of wave poynting flux: Powering the aurora. *Science*, *299*(5605), 383–386. https://doi.org/10.1126/science.1080073

Khurana, K., & Kivelson, M. G. (1989). Ultralow frequency MHD waves in Jupiter's middle magnetosphere. *Journal of Geophysical Research*, *94*(A5), 5241–5254. https://doi.org/10.1029/JA094iA05p05241

Khurana, K., Vasyliūnas, V., Mauk, B., Frank, L., Paterson, B., Kivelson, M., et al. (2004). The configuration of Jupiter's magnetosphere. *Jupiter: The Planet, Satellites and Magnetosphere*, 593–616.

Kimura, T., Cecconi, B., Zarka, P., Kasaba, Y., Tsuchiya, F., Misawa, H., & Morioka, A. (2012). Polarization and direction of arrival of Jovian quasiperiodic bursts observed by Cassini. *Journal of Geophysical Research*, *117*(A11). https://doi.org/10.1029/2012JA017506

Kimura, T., Tsuchiya, F., Misawa, H., Morioka, A., Nozawa, H., & Fujimoto, M. (2011). Periodicity analysis of Jovian quasi-periodic radio bursts based on Lomb-Scargle periodograms. *Journal of Geophysical Research*, *116*(A3). https://doi.org/10.1029/2010JA016076

Kronberg, E. A., Kasahara, S., Krupp, N., & Woch, J. (2012). Field-aligned beams and reconnection in the Jovian magnetotail. *Icarus*, *217*(1), 55–65. https://doi.org/10.1016/j.icarus.2011.10.011

Krupp, N., Woch, J., Lagg, A., Livi, S., Mitchell, D. G., Krimigis, S. M., et al. (2004). Energetic particle observations in the vicinity of Jupiter: Cassini MIMI/LEMMS results. *Journal of Geophysical Research*, *109*(A9). https://doi.org/10.1029/2003JA010111

Lorch, C. T. S., Ray, L. C., Wilson, R. J., Bagenal, F., Crary, F., Delamere, P. A., et al. (2022). Evidence of Alfvénic activity in Jupiter's mid-to-high latitude magnetosphere. *Journal of Geophysical Research: Space Physics*, *127*(6), e2021JA029853. https://doi.org/10.1029/2021JA029853

Lotko, W., Streltsov, A. V., & Carlson, C. W. (1998). Discrete auroral arc, electrostatic shock and suprathermal electrons powered by dispersive, anomalously resistive field line resonance. *Geophysical Research Letters*, *25*(24), 4449–4452. https://doi.org/10.1029/1998GL900200

Lysak, R. L. (2022). Field line resonances and cavity modes at Earth and Jupiter. *Frontiers in Astronomy and Space Sciences*, *9*, 913554. https://doi.org/10.3389/fspas.2022.913554

Lysak, R. L., & Song, Y. (2020). Field line resonances in Jupiter's magnetosphere. *Geophysical Research Letters*, *47*(18). https://doi.org/10.1029/2020GL089473

MacDowall, R. J., Kaiser, M. L., Desch, M. D., Farrell, W. M., Hess, R. A., & Stone, R. G. (1993). Quasiperiodic Jovian radio bursts: Observations from the Ulysses radio and plasma wave experiment. *Planetary and Space Science*, *41*(11), 1059–1072. https://doi.org/10.1016/0032-0633(93)90109-F

Manners, H., & Masters, A. (2019). First evidence for multiple-harmonic standing Alfvén waves in Jupiter's equatorial plasma sheet. *Geophysical Research Letters*, *46*(16), 9344–9351. https://doi.org/10.1029/2019GL083899

Manners, H., & Masters, A. (2020). The global distribution of ultralow-frequency waves in Jupiter's magnetosphere. *Journal of Geophysical Research: Space Physics*, *125*(10). https://doi.org/10.1029/2020JA028345

Mauk, B. H., Haggerty, D. K., Paranicas, C., Clark, G., Kollmann, P., Rymer, A. M., et al. (2017). Discrete and broadband electron acceleration in Jupiter's powerful aurora. *Nature*, *549*(7670), 66–69. https://doi.org/10.1038/nature23648

Montgomery, J., Ebert, R. W., Allegrini, F., Bagenal, F., Bolton, S. J., DiBraccio, G. A., et al. (2023). Investigating the occurrence of Kelvin-Helmholtz instabilities at Jupiter's dawn magnetopause. *Geophysical Research Letters*, *50*(14), e2023GL102921. https://doi.org/10.1029/2023GL102921

Nichols, J. D., Bunce, E. J., Clarke, J. T., Cowley, S. W. H., Gérard, J.-C., Grodent, D., & Pryor, W. R. (2007). Response of Jupiter's UV auroras to interplanetary conditions as observed by the Hubble Space Telescope during the Cassini flyby campaign. *Journal of Geophysical Research*, *112*(A2). https://doi.org/10.1029/2006JA012005

Nichols, J. D., Clarke, J. T., Gérard, J. C., Grodent, D., & Hansen, K. C. (2009). Variation of different components of Jupiter's auroral emission. *Journal of Geophysical Research*, *114*(A6). https://doi.org/10.1029/2009JA014051

Nichols, J. D., Yeoman, T. K., Bunce, E. J., Chowdhury, M. N., Cowley, S. W. H., & Robinson, T. R. (2017). Periodic emission within Jupiter's main auroral oval. *Geophysical Research Letters*, *44*(18), 9192–9198. https://doi.org/10.1002/2017GL074824

Pan, D., Yao, Z., Manners, H., Dunn, W., Bonfond, B., Grodent, D., et al. (2021). Ultralow-frequency waves in driving Jovian aurorae revealed by observations from HST and Juno. *Geophysical Research Letters*, *48*(5). https://doi.org/10.1029/2020GL091579

Rogers, A. J., Farrugia, C. J., Torbert, R. B., & Rogers, T. J. (2023). Applying magnetic curvature to MMS data to identify thin current sheets relative to tail reconnection. *Journal of Geophysical Research: Space Physics*, *128*(1), e2022JA030577. https://doi.org/10.1029/2022JA030577

Saur, J., Pouquet, A., & Matthaeus, W. H. (2003). An acceleration mechanism for the generation of the main auroral oval on Jupiter. *Geophysical Research Letters*, *30*(5). https://doi.org/10.1029/2002GL015761

Schok, A. A., Delamere, P. A., Mino, B., Damiano, P. A., Zhang, B., Sciola, A., et al. (2023). Periodicities and plasma density structure of Jupiter's dawnside magnetosphere. *Journal of Geophysical Research: Planets*, *128*(2). https://doi.org/10.1029/2022JE007637

Sinclair, J. A., Orton, G. S., Fernandes, J., Kasaba, Y., Sato, T. M., Fujiyoshi, T., et al. (2019). A brightening of Jupiter's auroral 7.8-μm CH4 emission during a solar-wind compression. *Nature Astronomy*, *3*(7), 607–613. https://doi.org/10.1038/s41550-019-0743-x

Southwood, D. J., & Kivelson, M. G. (1987). Magnetospheric interchange instability. *Journal of Geophysical Research*, *92*(A1), 109–116. https://doi.org/10.1029/JA092iA01p00109

Southwood, D. J., & Kivelson, M. G. (2001). A new perspective concerning the influence of the solar wind on the Jovian magnetosphere. *Journal of Geophysical Research*, *106*(A4), 6123–6130. https://doi.org/10.1029/2000JA000236

Torrence, C., & Compo, G. P. (1998). A practical guide to wavelet analysis. *Bulletin of the American Meteorological Society*, *79*(1), 61–78. https://doi.org/10.1175/1520-0477(1998)079<0061:APGTWA>2.0.CO;2

Vogt, M. F., Connerney, J. E. P., DiBraccio, G. A., Wilson, R. J., Thomsen, M. F., Ebert, R. W., et al. (2020). Magnetotail reconnection at Jupiter: A survey of Juno magnetic field observations. *Journal of Geophysical Research: Space Physics*, *125*(3). https://doi.org/10.1029/2019JA027486

Watanabe, H., Kita, H., Tao, C., Kagitani, M., Sakanoi, T., & Kasaba, Y. (2018). Pulsation characteristics of Jovian infrared northern aurora observed by the Subaru IRCS with adaptive optics. *Geophysical Research Letters*, *45*(21), 11547–11554. https://doi.org/10.1029/2018GL079411

Weigt, D. M., Jackman, C. M., Dunn, W. R., Gladstone, G. R., Vogt, M. F., Wibisono, A. D., et al. (2020). Chandra observations of Jupiter's X-ray auroral emission during Juno Apojove 2017. *Journal of Geophysical Research: Planets*, *125*(4). https://doi.org/10.1029/2019JE006262

Wibisono, A. D., Branduardi-Raymont, G., Dunn, W. R., Coates, A. J., Weigt, D. M., Jackman, C. M., et al. (2020). Temporal and spectral studies by XMM-Newton of Jupiter's X-ray auroras during a compression event. *Journal of Geophysical Research: Space Physics*, *125*(5). https://doi.org/10.1029/2019JA027676

Wibisono, A. D., Branduardi-Raymont, G., Dunn, W. R., Kimura, T., Coates, A. J., Grodent, D., et al. (2021). Jupiter's X-ray aurora during UV dawn storms and injections as observed by XMM–Newton, Hubble, and Hisaki. *Monthly Notices of the Royal Astronomical Society*, *507*(1), 1216–1228. https://doi.org/10.1093/mnras/stab2218

Xu, Y., Yao, Z. H., Zhang, B., Delamere, P. A., Ray, L. C., Dunn, W. R., et al. (2023). On the relation between Jupiter's aurora and the dawnside current sheet. *Geophysical Research Letters*, *50*(13), e2023GL104123. https://doi.org/10.1029/2023GL104123

Yao, Z., Dunn, W. R., Woodfield, E. E., Clark, G., Mauk, B. H., Ebert, R. W., et al. (2021). Revealing the source of Jupiter's x-ray auroral flares. *Science Advances*, *7*(28), eabf0851. https://doi.org/10.1126/sciadv.abf0851

Yao, Z. H., Bonfond, B., Grodent, D., Chané, E., Dunn, W. R., Kurth, W. S., et al. (2022). On the relation between auroral morphologies and compression conditions of Jupiter's magnetopause: Observations from Juno and the Hubble Space telescope. *Journal of Geophysical Research: Space Physics*, *127*(10). https://doi.org/10.1029/2021JA029894

Yao, Z. H., Grodent, D., Ray, L. C., Rae, I. J., Coates, A. J., Pu, Z. Y., et al. (2017). Two fundamentally different drivers of dipolarizations at Saturn. *Journal of Geophysical Research: Space Physics*, *122*(4), 4348–4356. https://doi.org/10.1002/2017JA024060

Zarka, P., & Genova, F. (1983). Low-frequency Jovian emission and solar wind magnetic sector structure. *Nature*, *306*(5945), 767–768. https://doi.org/10.1038/306767a0

Zhang, B., Delamere, P. A., Ma, X., Burkholder, B., Wiltberger, M., Lyon, J. G., et al. (2018). Asymmetric Kelvin-Helmholtz instability at Jupiter's magnetopause boundary: Implications for corotation-dominated systems. *Geophysical Research Letters*, *45*(1), 56–63. https://doi.org/10.1002/2017GL076315

Zong, Q., Rankin, R., & Zhou, X. (2017). The interaction of ultra-low-frequency pc3-5 waves with charged particles in Earth's magnetosphere. *Reviews of Modern Plasma Physics*, *1*(1), 10. https://doi.org/10.1007/s41614-017-0011-4